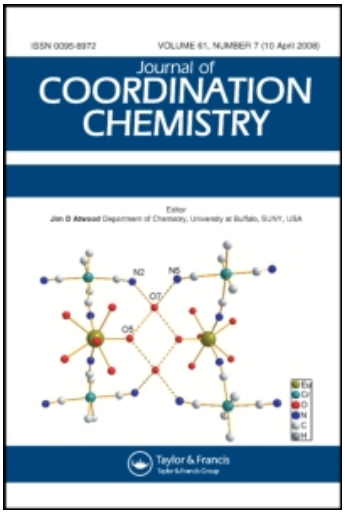

Journal of Coordination Chemistry
Publication details, including instructions for authors and subscription information:
http://www.informaworld.com/smpp/title~content=t713455674

Kinetic Studies of the Fe(III)/DI-2-Pyridyl Ketone Benzoylhydrazone Complex Reduction By Sulfite

Cristiane F. F. Lopes[a]; Nina Coichev[a]; Maria E. V. Suárez-Iha[a]
[a] Instituto de Química, Universidade de São Paulo, São Paulo, SP, Brazil

Online publication date: 15 September 2010

To cite this Article Lopes, Cristiane F. F. , Coichev, Nina and Suárez-Iha, Maria E. V.(2002) 'Kinetic Studies of the Fe(III)/DI-2-Pyridyl Ketone Benzoylhydrazone Complex Reduction By Sulfite', Journal of Coordination Chemistry, 55: 9, 1029 — 1042
To link to this Article: DOI: 10.1080/0095897021000009992
URL: http://dx.doi.org/10.1080/0095897021000009992

J. Coord. Chem., 2002, Vol. 55(9), pp. 1029–1044

Taylor & Francis
Taylor & Francis Group

KINETIC STUDIES OF THE Fe(III)/DI-2-PYRIDYL KETONE BENZOYLHYDRAZONE COMPLEX REDUCTION BY SULFITE

CRISTIANE F.F. LOPES, NINA COICHEV and MARIA E.V. SUÁREZ-IHA*

Instituto de Química, Universidade de São Paulo, C.P. 26077 CEP 05513-970, São Paulo, SP, Brazil

(Received 4 January 2001; Revised 21 August 2001; In final form 14 January 2002)

The reactions of HSO_3^- with Fe(III) in the presence of di-2-pyridyl ketone benzoylhydrazone (DPKBH) have been investigated at 4.2–7.2 pH. The decomposition reaction of Fe(III)/DPKBH has been studied as a function of total sulfite concentration using spectrophotometric techniques. The kinetics are controlled by the equilibrium $[Fe^{III}(DPKBH)(H_2O)]^{2+} \rightleftharpoons [Fe^{III}(DPKBH)(OH)]^{+} + H^{+}$, for which the hydrolysis constant was potentiometrically determined as 4.3×10^{-5} M, at $(25.0 \pm 0.1)^{\circ}$C and 1.5×10^{-3} M ionic strength. Both of those species undergo sulfite substitution and the significantly more labile species is the aqua complex. The formation constants of $[Fe^{III}(DPKBH)(SO_3)]$ are 1.2×10^4 at pH 4.2 and $1.9 \times 10^2\,M^{-1}$ at pH 6.2. The limiting rate constants, k, at high HSO_3^- concentrations are $3.5 \times 10^{-2}\,s^{-1}$ and $1.4 \times 10^{-2}\,s^{-1}$, respectively, at pH 4.2 and 6.2, $I = 1.3 \times 10^{-2}$ M. The results are discussed with reference to the available literature data.

Keywords: Iron; Sulfite; Di-2-pyridyl ketone benzoylhydrazone; Kinetics; Sulfur(IV)

INTRODUCTION

Pehkonen *et al.* [1] proposed a new analytical method for simultaneous spectrophotometric determination of Fe(II) and Fe(III) in atmospheric water. The effect of S(IV) (0.1 M) was investigated at pH 3.5 and 6.2 in room light and in the dark; its presence affects the iron(II) and iron(III) concentration since S(IV) is a good reducing agent. The dependence of the reduction rate on pH suggests different mechanisms. Formaldehyde addition, at pH 3.5, showed no effect on the reaction rate, which means that a (S(IV)–HCHO) adduct did not prevent Fe(III) reduction. As a result those authors [1] concluded that the absorbance readings should be taken immediately, 2–5 min, after sampling and reagent addition, in order to know the oxidation state of the iron ion in the sample at the time of collection.

Di-2-pyridyl ketone benzoylhydrazone (DPKBH) is a multidentade ligand and is a sensitive reagent (1) used for the spectrophotometric determination of trace amounts of many transition metal ions and for analysis of iron(II) [2], iron(II) and iron(III) [3], cobalt(II) [4], palladium(II) [5] and nickel(II) [6,7]. The concentrations of Fe(II)

*Corresponding author. Fax: (55) (011) 3815 5579. E-mail: maevsiha@iq.usp.br

ISSN 0095-8972 print: ISSN 1029-0389 online © 2002 Taylor & Francis Ltd
DOI: 10.1080/0095897021000009992

and Fe(III) were also simultaneously determined in cloudwater samples by a spectrophotometric technique employing DPKBH as a dual chelating agent [1].

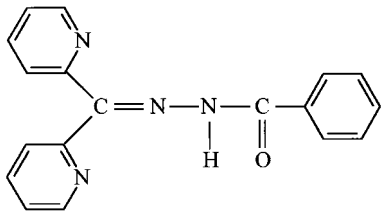

(1)

di-2-pyridyl ketone benzoylhydrazone (DPKBH)

In the present study we have investigated the kinetics and mechanism of the Fe(III)/DPKBH reduction by HSO_3^-, in the absence of oxygen, by following the spectral absorbance changes. The combination of the reduction reaction and acid–base equilibrium studies is reported.

EXPERIMENTAL

All reagents were of analytical grade (Merck or Aldrich Chemical) and deionized water was used to prepare all solutions. Nitrogen was used to deaerate all solutions and solvents before mixing.

Stock solutions of sulfite (0.010 M) were prepared daily by dissolving $Na_2S_2O_5$ in deaerated water. The hydrolysis of one mol of metabisulfite ion gives two mols of bisulfite and, the pH of the final solution is close to 4.5, which is much better than the pH 9 relative to a solution prepared from a sulfite salt. The concentration was determined using the iodometric method, by acidification of an aliquot with acetic acid followed by back titration of the excess iodine with thiossulfate [8].

A standard solution of iron(III) perchlorate (0.010 M) was prepared by dissolving reagent-grade iron(III) perchlorate in water and perchloric acid. The final pH was adjusted to 1 in order to avoid the hydrolysis of the metal ion and the iron(III) concentration was determined by titration with a standard EDTA solution in the presence of a Variamin Blue indicator [8].

The synthesis of DPKBH was performed according to the procedure outlined by Garcia-Vargas *et al.* [9]. After synthesis, the melting point of the product was verified to be 134°C and its absorption spectrum was checked and compared with previously reported values [9]. The DPKBH stock solution 0.010 M was prepared in 5% ethanol and may be stored for 30 days.

Working Solutions The acidity of the working solutions was adjusted at pH 4.2, 4.7 and 5.7 with CH_3COOH/CH_3COO^- buffer solution; at pH 6.2 with ammonium acetate and at pH 7.1 with TRIS/$HTRIS^+$ (2-amino-2-hydroxymethyl 1,3-propanediol).

The final working solutions were prepared by mixing appropriate volumes of the stock solutions in the following order: Fe(III), DPKBH/ethanol and buffer. DPKBH solution was prepared in 5% of ethanol because of the low solubility of the ligand [9] in water.

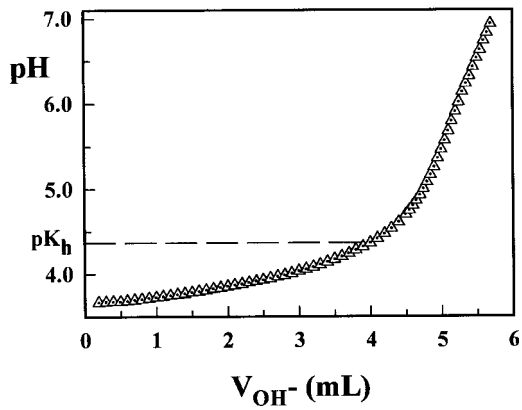

FIGURE 1 pH titration of 25.0 mL of 1.0×10^{-4} M $[Fe^{III}(DPKBH)]^{2+}$ with 1.75×10^{-3} M NaOH at 25°C and $I = 1.5 \times 10^{-3}$ M.

After the addition of a very small volume, μL, of HSO_3^- solution (to avoid dilution) to the working solution the formation of $[Fe^{II}(DPKBH)_n]^{2-n}$ was followed by absorbance changes at 360 and 640 nm. In all figures the composition of the final solutions after mixing are indicated.

Due to the low solubility of the Fe^{II}/DPKBH complexes, the iron(II) concentration was kept constant (2.0×10^{-5} M). All final solutions were prepared in 25.0 mL plastic volumetric flasks because of the strong adsorption of DPKBH onto glass materials. The spectrophotometric quartz cell was washed with diluted nitric acid solution followed by water.

The UV–VIS spectra were recorded on an HP 8452 spectrophotometer, which was also used for kinetic measurements in the thermostated (25.0 ± 0.1)°C cell compartment. All UV–VIS spectra were recorded using the proper DPKBH concentration and the buffer in 5% ethanol as a blank solution and a spectrophotometric cell of 1.00 cm optical pathlength.

The potentiometric titration was carried out with a 5% ethanol solution of $[Fe^{III}(DPKBH)]^{2+}$ prepared from a mixture of the components Fe(III) and DPKBH in a ratio 1 : 1. For accurate pH measurements, the known acidity of the metal ion stock solution was partially neutralized with a more concentrated NaOH solution, such that the initial pH of the titrated solution was 3.6 (Fig. 1). Sodium perchlorate (Merck) was used to adjust the ionic strength (I) of the test solution, whereas NaOH and $HClO_4$ were used to adjust the pH. The potentiometric measurements were carried out in a 5 mL Metrohm 6.1418.150 thermostated jacketed cell at (25.0 ± 0.1)°C. The pH was measured on a Metrohm 654 pHmeter equipped with a Metrohm glass electrode of which the Ag/AgCl reference was filled with 3 M NaCl.

RESULTS AND DISCUSSION

Properties of DPKBH

Di-2-pyridyl ketone benzoylhydrazone was formerly synthesized by Nakanishi and Otomo [2] and it is a soluble reagent in different organic solvents but slightly soluble in water.

In aqueous-ethanolic solutions, DPKBH has many protonated forms at different pH values [2]. In acid solutions the pyridine nitrogen atom (RN) can be protonated (RNH^+) according to the following equilibrium:

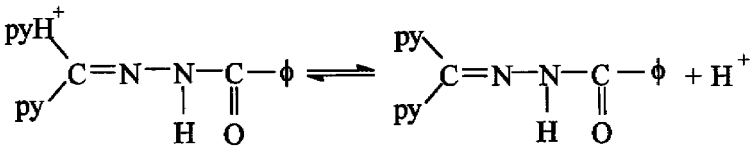

$$RNH^+ \rightleftharpoons RN + H^+ \qquad (K_1) \qquad (2)$$

We shall consider the protonated form of the ligand (pyridine nitrogen) as RNH^+, Eq. (**2**), and the neutral ligand as RN Eq. (**2**). The last form will be also represented as ROH when the ligand is considered in equilibrium with the anionic deprotonated form, RO^-, which corresponds to deprotonation of the $-COH$ group from the enolic form, according to the following equilibria, Eqs. (**3**) and (**4**). The symbol ϕ, Eq. (**3**), represents the phenyl group.

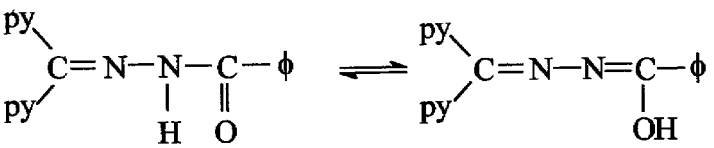

(cetonic form) (enolic form) (3)

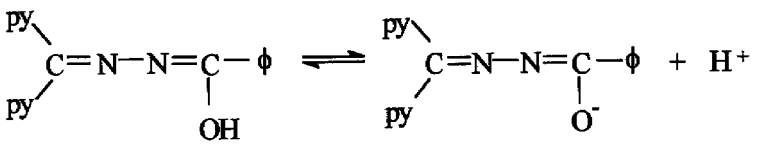

$$ROH \rightleftharpoons RO^- + H^+ \qquad (K_2) \qquad (4)$$

In 10% ethanolic solutions, DPKBH has a pK_1 of 3.21 and pK_2 of 10.8 [10]. Although the dissociation of a proton from the neutral DPKBH molecule is not favorable under the conditions of our experiments (pH 4.2–7.2), enhancement of its acidity after metal complex formation may promote its dissociation and coordination as an anion (RO^-).

Properties of Fe(II)/DPKBH and Fe(III)/DPKBH Complexes

The spectral characteristics of Fe(II)/DPKBH and Fe(III)/DPKBH complexes depend on the solution acidity and the ethanol percentage [9,11].

The molar absorptivities for the Fe(III)/DPKBH and Fe(II)/DPKBH complexes were calculated from absorbance measurements obtained with solutions prepared by the addition of iron ions (1.0×10^{-5} M) to DPKBH in excess (1.0×10^{-4} M), in 5% ethanol and, at the indicated pH. More details about the properties of these complexes and the ligand can be found in [9–11].

Stability constants and molar absorptivities for Fe(II) and Fe(III) complexes are summarized in Table I. Conductivity studies and the IR spectrum have clearly shown that DPKBH exists in the enolic form, exhibits tridentate behavior and is co-ordinated to iron in the anionic form [11].

With the stability constants (Table I) of the Fe(III)/DPKBH complexes the distribution diagram of the species is presented in Fig. 2. In the present work, the kinetics studies were performed with 1.0×10^{-4} M DPKBH which represents excess with respect to the Fe^{3+} concentration. In such conditions the percentages of the species $[Fe^{III}(RO)]^{2+}$ and $[Fe^{III}(RO)_2]^{+}$ are 70 and 30%, respectively. Additionally, we need to consider the acid–base equilibrium Eq. (**5**):

$$[Fe^{III}(RO)(H_2O)]^{2+} \rightleftharpoons [Fe^{III}(RO)(OH)]^{+} + H^{+} \quad (K_h) \tag{5}$$

TABLE I Stability constants (in 50% ethanol) [11] and molar absorptivities ($mol^{-1}\,cm\,L^{-1}$) (in 5% ethanol) of Fe(II)/DPKBH and Fe(III)/DPKBH complexes

	Fe(II)/DPKBH	*Fe(III)/DPKBH*
β_1	$1.22 \times 10^5\,M^{-1}$	$4.69 \times 10^6\,M^{-1}$
β_2	$7.81 \times 10^9\,M^{-2}$	$2.20 \times 10^{10}\,M^{-2}$
ε* (360 nm)	1.3×10^4 (pH 4.2)	1.8×10^4 (pH 4.2)
	2.5×10^4 (pH 6.2)	1.2×10^4 (pH 6.2)
ε* (640 nm)	0.73×10^4 (pH 6.2)	–

*present work.

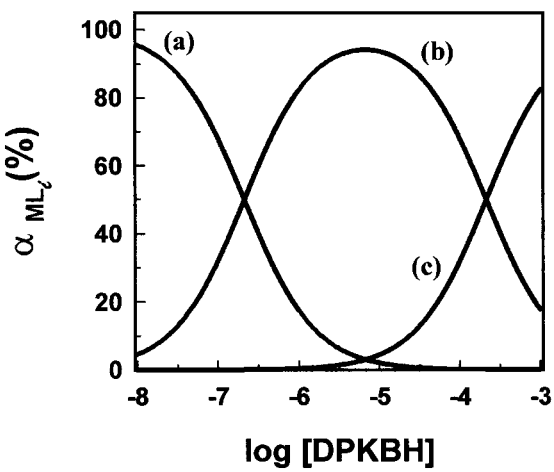

FIGURE 2 Distribution diagram for the species (a, b and c) present in the system Fe(III)/DPKBH [11]. $T = (25.0 \pm 0.1)^{\circ}C$, pH = (5.30 ± 0.1), and 50% ethanol. (a) ≡ Fe(III); (b) ≡ $[Fe^{III}(RO)]^{2+}$ and (c) ≡ $[Fe^{III}(RO)_2]^{+}$.

In a series of experiments the acid–base properties of the $[Fe^{III}(RO)(H_2O)]^{2+}$ complex were investigated by potentiometric titration of 1:1 mixtures of Fe^{3+} and DPKBH with sodium hydroxide solution. A typical example of such a titration curve is given in Fig. 1. The formation of $Fe(OH)_3$ was observed above pH 7. At the stoichiometric point (pH 5.8) the ratio 2:1 for $[OH^-]_{added}:[Fe^{III}(DPKBH)^{2+}]$ was found and it can be interpreted considering two acid–base equilibria according to Eqs. (**4**) and (**5**). The K_h value was calculated from the plot of the experimental pH *vs.* $\log\{[Fe^{III}(RO)(OH)^+]/[Fe^{III}(RO)(H_2O)^{2+}]\}$ according to the Henderson–Hassellbach [12] equation:

$$pH = pK_h + \log\frac{[Fe(RO)(OH)^+]}{[Fe(RO)(H_2O)^{2+}]} \tag{6}$$

The average K_h value, from triplicate titrations, was $(4.3 \pm 0.1) \times 10^{-5}$ M ($I = 1.5 \times 10^{-3}$ M, $T = 25.0°C$).

Additional evidence on the acid–base equilibrium in solution comes from UV–VIS spectra (Fig. 3) recorded as a function of pH. These spectra are relative to a mixture of several species in solution: $[Fe^{III}(RO)(H_2O)]^{2+}$, $[Fe^{III}(RO)(OH)]^+$, $[Fe^{III}(RO)_2]^+$, since they were obtained at 1.0×10^{-4} M DPKBH (see Fig. 2). On gradually increasing the pH, the absorbance maximum shifts to higher wavelength with an isobestic point at 385 nm. These spectral changes can be ascribed to deprotonation of $[Fe^{III}(RO)(H_2O)]^{2+}$ to produce $[Fe^{III}(RO)(OH)]^+$ during the increase in pH (4.2–7.1). The observed increase in absorbance in the 410–450 nm region can be attributed to an increase of the concentration of $[Fe^{III}(RO)(OH)]^+$ species.

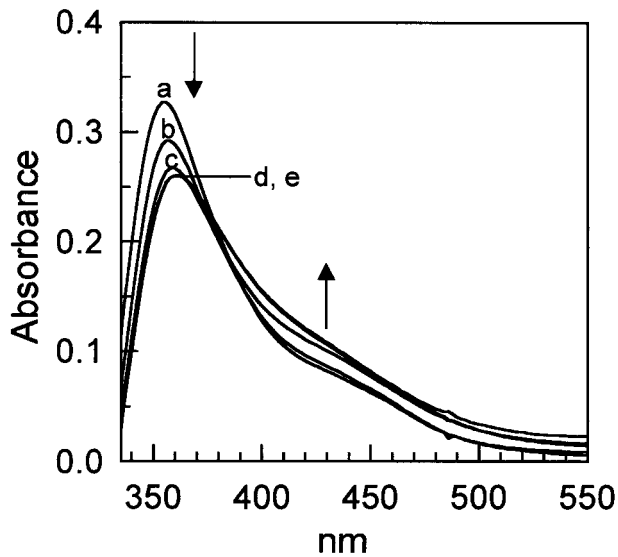

FIGURE 3 Spectra of Fe(III)/DPKBH solutions at different pH: (a) 4.2; (b) 4.7; (c) 5.1; (d) 6.2 and (e) 7.1. Conditions: $[Fe^{III}(DPKBH)_2]^+ = 2.0 \times 10^{-5}$ M; DPKBH $= 1.0 \times 10^{-4}$ M; optical path length = 1.00 cm.

Kinetic Measurements

The interpretation of the kinetic data is very complex since different species are present according to the acidity and ligand concentration. The percentages of such species, calculated with the global stability constants [11] (Table I) at 1.0×10^{-4} M DPKBH, are 70 and 30% for $[Fe^{III}(RO)H_2O]^{2+}$) and ($[Fe^{III}(RO)_2]^{+}$), respectively (Fig. 2).

All calculations, in this work, were done considering only the results obtained in experimental conditions of 1.0×10^{-4} M DPKBH, because the percentage of the $[Fe^{III}(RO)_2]^{+}$ species increases with ligand concentration. In this way, we limited the calculations considering the data where the $[Fe^{III}(RO)]^{2+}$ was the predominant species in solution. The k_{obs} data at higher DPKBH concentrations are represented in Fig. 6.

The combination of all possibilities, of species present according to the different acidity and ligand concentration, results in the scheme outlined in Eq. (**7**) showing the possible reactive species in solution.

$$\begin{matrix}[Fe^{III}(RO)(H_2O)]^{2+} \\ [Fe^{III}(RO)(OH)]^{+} + HSO_3^- \rightleftharpoons [Fe^{II}(RO)_n]^{2-n} + SO_4^{2-} + S_2O_6^{2-} \\ [Fe^{III}(RO)_2]^{+}\end{matrix} \quad (7)$$

(a) pH Dependence

In the present study, the Fe(III) reduction was followed when (0.2 to 1.4) $\times 10^{-3}$ M HSO_3^- was added to a solution of Fe(III) 2.0×10^{-5} M, DPKBH (1.0–3.0) $\times 10^{-4}$ M, pH 4.2–7.1 in 5% ethanol under anaerobic conditions, where HSO_3^- was always in large excess compared to Fe(III)/DPKBH. After addition of HSO_3^- solution, the Fe(II) formation was followed by the absorbance changes at 360 and 640 nm.

Figure 4 shows the successive spectra at pH 6.2 showing the reduction of Fe(III) by HSO_3^-. The absorbance increases at 360 and 640 nm, ascribed to the higher molar

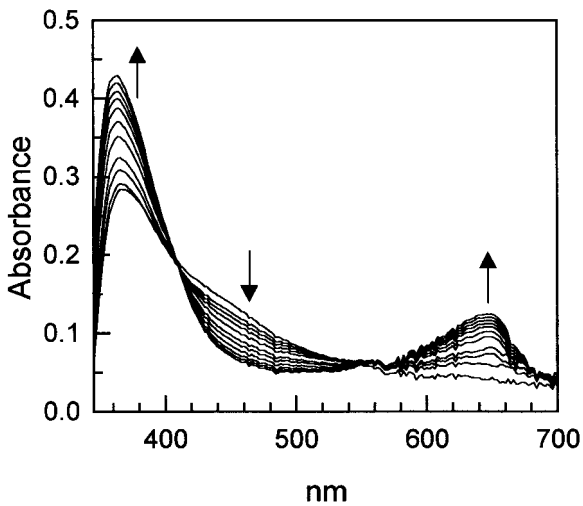

FIGURE 4 UV–VIS spectra after the addition of HSO_3^- 2.0×10^{-3} M to a Fe(III)/DPKBH solution. Conditions: $[Fe^{III}(DPKBH)_2]^{+} = 2.0 \times 10^{-5}$ M; DPKBH = 1.0×10^{-4} M; pH 6.2 (NH_4Ac). $I = 1.3 \times 10^{-2}$ M. $T = 25.0^{\circ}C$, optical path length = 1.00 cm.

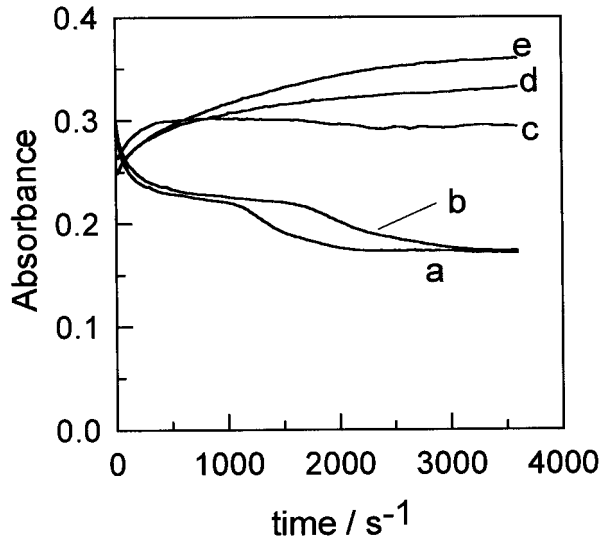

FIGURE 5 Absorbance changes at 360 nm after the addition of 6×10^{-4} M HSO_3^- to a Fe(III)/DPKBH solution at different pH: (a) 4.2; (b) 4.7; (c) 5.1; (d) 6.2 and (e) 7.1. Conditions: $[Fe^{III}(DPKBH)_2]^+ = 2.0 \times 10^{-5}$ M; DPKBH $= 1.0 \times 10^{-4}$ M. $T = 25.0°C$; optical path length = 1.0 cm.

absorptivity of the Fe(II) complexes compared to Fe(III) (Table I). The absorbance decreasing in the 410–450 nm region makes evident the significant decrease of $[Fe^{III}(RO)(H_2O)]^{2+}$ and $[Fe^{III}(RO)(OH)]^+$ concentrations.

Figure 5 shows the absorbance changes at 360 nm after addition of HSO_3^- to Fe(III) complex solutions at different acidities. The profile of the absorbance changes can be explained by the relative values of the molar absorptivities (ε) of the Fe(II) and Fe(III) complexes at different pH (Table I); that is, at pH 4.2 ε (Fe(II)/DPKBH) is lower than ε (Fe(III)/DPKBH) and at pH 6.2 the opposite relationship is observed.

The Olis Kinfit programs [13] were used to fit the absorbance-time traces of Fig. 5 consecutive first-order reactions, leading to k_{obs1} and k_{obs2}. The total time of 1200 s was considered for the data obtained at pH 4.2; 4.7 and 5.1 that is, only the first step. However, for pH 6.2 and 7.1 the total time used was 3600 s. At pH 4.2 (Fig. 5(a) and 4.7 (Fig. 5(b)) there is a second reaction which is probably decomposition of the Fe(II) complex.

The molar absorptivities of the Fe(II) and Fe(III) complexes are strongly dependent on the solution acidity. Considering the ε values in Table I and the respective absorbance values for the solutions at pH 4.2 (at 1200 s) and pH 6.2 (at 3600 s), the percentages of Fe(III) reduction to Fe(II) complex were calculated. Using the S(IV) concentrations, indicated in Fig. 5, these calculated percentages were 37–53 at pH 4.2 and 15–50 at pH 6.2, showing a non-quantative reduction at those time intervals.

In these time intervals, the reduction of Fe(III) to Fe(II) showed an initial, faster step followed by parallel or consecutive reactions involving the formation of an $[Fe^{III}(RO)(SO_3)]$ intermediate followed by $[Fe^{II}(RO)_2]$, SO_4^{2-} and other sulfur compounds resulting from the radical $SO_3^{\bullet -}$ parallel reaction.

The average k_{obs1} and k_{obs2} values are represented in Fig. 6. For the mechanism we only consider the relationship of k_{obs1} with the acidity and $[HSO_3^-]$. Because the system is very complex, it is difficult to interpret the data based on the k_{obs2} values.

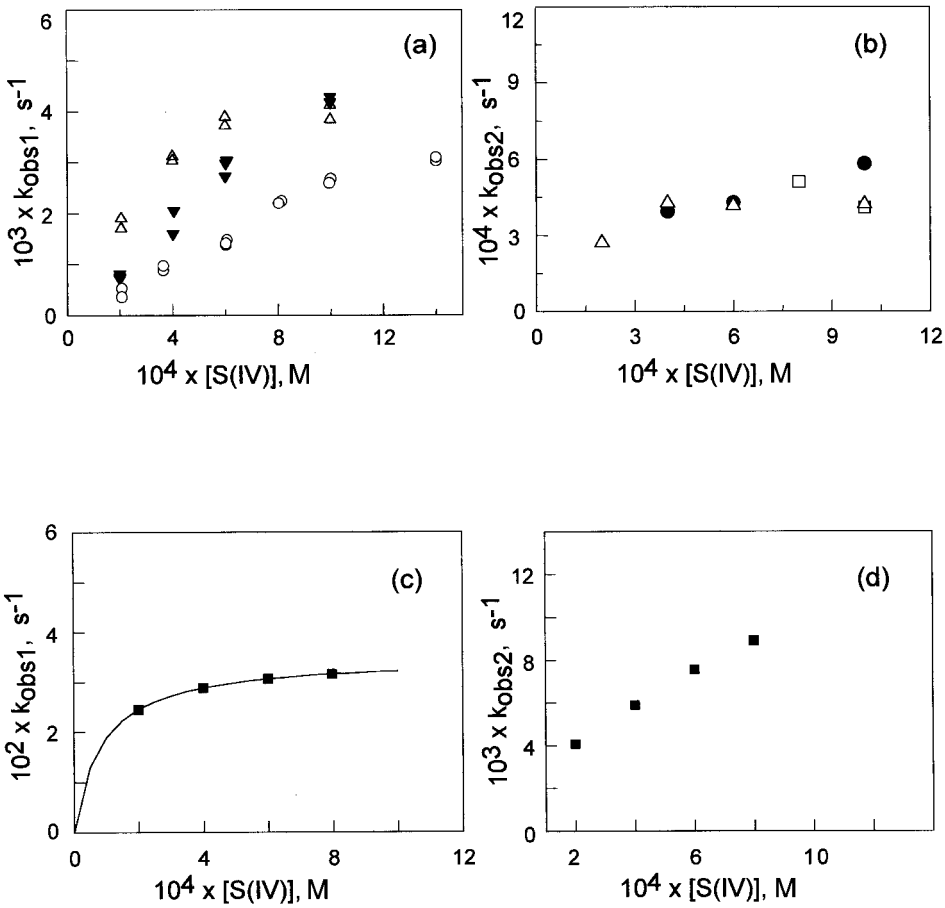

FIGURE 6 Rate constants k_{obs1} (a,c) and k_{obs2} (b,d) as a function of HSO_3^- concentration at pH 6.2 (a,b) and 4.2 (c,d). Conditions: $Fe^{3+} = 2.0 \times 10^{-5}$ mol/L; $T = 25.0°C$; $\lambda = 360$ nm; DPKBH (a) = [○] 1.0×10^{-4}, [Δ] 2.0×10^{-4}, [▼] 3.0×10^{-4} M; (b) = [□] 1.0×10^{-4}, [●] 2.0×10^{-4}, [Δ] 3.0×10^{-4} M and (c,d) = 1.0×10^{-4} M.

Different average values of k_{obs1} as a function of pH can be explained by the characteristic acid–base equilibrium of Fe(III)/DPKBH (Eq. 5). To relate the different reactivity of $[Fe^{III}(RO)(OH)]^+$ and $[Fe^{III}(RO)(H_2O)]^{2+}$ at different pH, the molar fractions of each species were calculated using the following equations:

$$\alpha = [Fe^{III}(RO)(OH)^+]/C_{Fe(III)} = K_h/([H^+] + K_h), \quad \text{for} \quad [Fe^{III}(RO)(OH)]^+ \tag{8}$$

$$\alpha' = [Fe^{III}(RO)(H_2O)^{2+}]/C_{Fe(III)} = [H^+]/([H^+] + K_h), \quad \text{for} \quad [Fe^{III}(RO)(H_2O)]^{2+} \tag{9}$$

where $C_{Fe(III)}$ is the total Fe(III) concentration.

Figure 7 clearly shows the different reactivity of $[Fe^{III}(RO)(OH)]^+$ and $[Fe^{III}(RO)(H_2O)]^{2+}$ species at different pH. The decreasing of k_{obs1} is in excellent agreement with the molar fractions of the $[Fe^{III}(RO)(H_2O)]^{2+}$ species. On the other hand, the dependence between k_{obs1} and the pH cannot be ascribed to the acid–base equilibria of

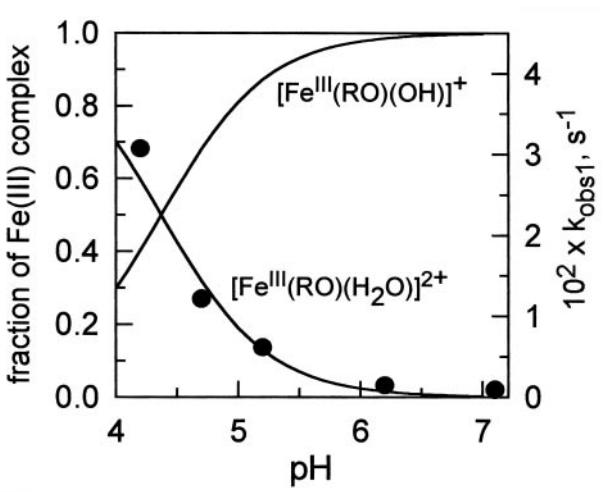

FIGURE 7 Distribution diagram (—) of the two species considering the acid-base equilibrium of the Fe(III)/DPKBH complexes and the experimental k_{obs1} values (●). DPKBH = 1.0×10^{-4} M; Fe(III) = 2.0×10^{-5} M; $HSO_3^- = 6.0 \times 10^{-4}$ M.

S(IV) and ligand species, since in the pH range (4.2–6.2) the neutral ligand (RN) and HSO_3^- are the predominate species.

The data plotted in Fig. 7 show the higher reactivity of the $[Fe^{III}(RO)(H_2O)]^{2+}$ complex. Evidence of the presence of at least two distinct species can be inferred from Fig. 3, by the isobestic point at 385 nm.

(b) HSO_3^- Concentration Dependence

In the following kinetic data treatment we have supposed the formation of a mixed complex of Fe(III) with DPKBH and sulfite. $[Fe^{III}(RO)_2]^+$ was not considered since it is not significant (at 1.0×10^{-4} M DPKBH) and the coordination sites of the Fe(III) center are occupied; formation of the respective mixed complex is not favorable.

Considering the existence of a pre-equilibrium step leading to the formation of $[Fe^{III}(RO)(SO_3)]$ which is rapid compared to the reduction of Fe(III), for example at pH 4.2, the rate equation is:

$$\frac{d[Fe^{II}(RO)_2]}{dt} = -d\{[Fe^{III}(RO)(H_2O)]^{2+} + [Fe^{III}(RO)(SO_3)]\}/dt$$

$$= k[Fe^{III}(RO)(SO_3)] \quad (10)$$

$$[HSO_3^-] \gg [Fe^{III}(RO)(H_2O)^{2+}] \quad (11)$$

Expressing $[Fe^{III}(RO)(SO_3)]$ in terms of $[Fe^{III}(RO)(H_2O)^{2+}]$ and $[HSO_3^-]$, considering the equilibrium constant (Eq. **12**)

$$K = \frac{[Fe^{III}(RO)(SO_3)]}{[Fe^{III}(RO)(H_2O)^{2+}][HSO_3^-]} \quad (12)$$

and assuming that $[Fe^{III}(RO)(SO_3)]$ is fraction of total Fe(III):

$$[Fe^{III}(RO)(SO_3)] = \frac{K[HSO_3^-]}{1 + K[HSO_3^-]} \cdot \{[Fe^{III}(RO)(H_2O)^{2+}] + [Fe^{III}(RO)(SO_3)]\} \quad (13)$$

The combination of Eqs. (**10**) and (**13**) gives:

$$\frac{d[Fe^{II}(RO)_2]}{dt} = \frac{kK \cdot [HSO_3^-]}{1 + K \cdot [HSO_3^-]} \cdot \{[Fe^{III}(RO)(H_2O)^{2+}] + [Fe^{III}(RO)(SO_3)]\} \quad (14)$$

and

$$k_{obs} = \frac{kK \cdot [HSO_3^-]}{1 + K \cdot [HSO_3^-]} \quad (15)$$

or

$$k_{obs}^{-1} = k^{-1} + \{kK\,[HSO_3^-]\}^{-1} \quad (16)$$

The Eq. (**16**) is consistent with the linearity of the plot in Fig. 8. The values of k and K were deduced from the least-square values of the intercepts ($= 1/k_{obs}$) and the slopes ($1/k_{obs}K$), Fig. 8.

Experiments at HSO_3^- concentrations lower than 2×10^{-4} M would better define the curves shown in Fig. 6, (especially in Fig. 6(c)) however, the absorbance changes at lower concentrations had large uncertainties. Because of the lack of sufficiently detailed experimental information, the treatment of the kinetic data yields a semiquantiative description to estimate the kinetic constants. In the present work it was possible to determine the main pathways in the intrinsic mechanism, since several iron complexes are present.

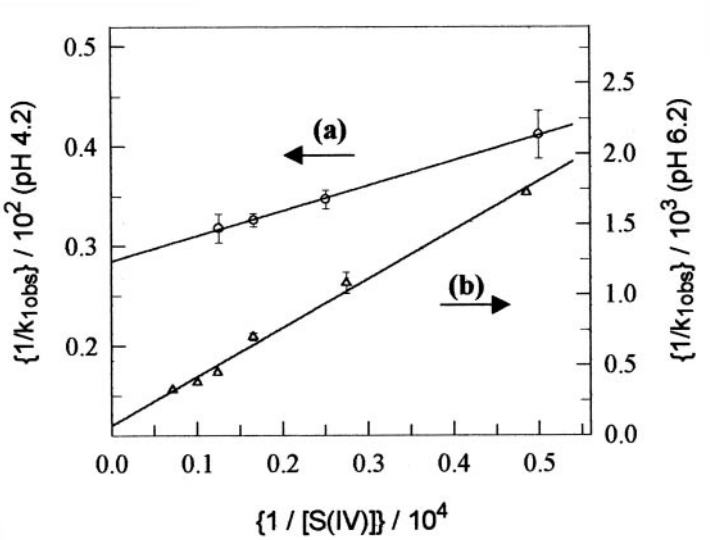

FIGURE 8 Rate constant reciprocals ($1/k_{obs1}$) as a function of the HSO_3^- concentration reciprocal at pH 4.2 (a) and 6.2 (b). Conditions: $Fe^{3+} = 2.0 \times 10^{-5}$ M; $T = 25.0°C$; DPKBH $= 1.0 \times 10^{-4}$ M.

Similar considerations can be done at pH 6.2 where $[Fe^{III}(RO)(OH)^{+}]$ is the major species.

The results from the rate measurements carried out at pH 4.2 and 6.2 are presented in the sequence of reaction shown in schemes (**17**) and (**18**), respectively.

(b.1) HSO_3^- Concentration Dependence at pH 4.2

The suggested mechanism based on the pH dependence shows the aqua complex, which is predominant at pH 4.2, as the main reactive species (Fig. 7). Based on this, the following scheme can be outlined, in Eq. (**17**).

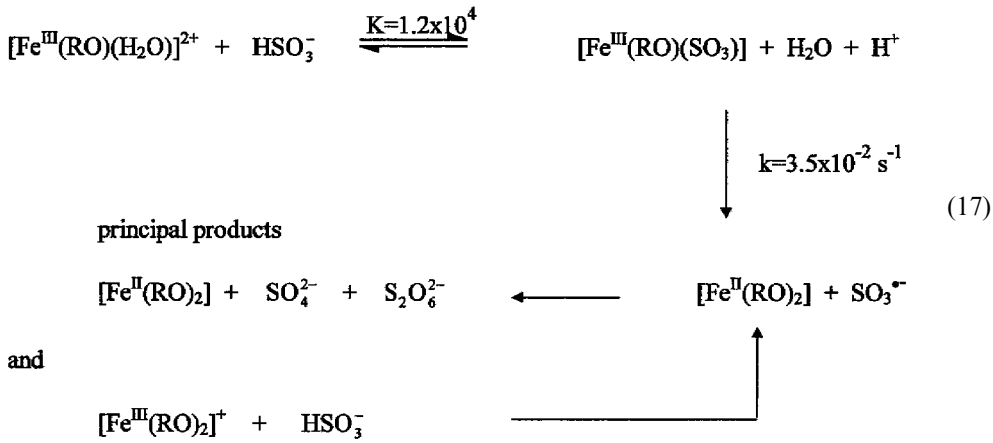

SCHEME 1 (pH = 4.2).

For the mechanism in Eq. (**17**), the appropriate rate expression is Eq. (**14**) which involves one pre-equilibrium step.

Under these conditions the limiting rate constant at high HSO_3^- concentration should be k, Fig. 6(c), and a plot of $1/k_{obs1}$ *vs.* $1/[HSO_3^-]$ is linear with intercept $1/k$ and slope $1/(kK)$. For 1.0×10^{-4} M DPKBH and pH 4.2 the average values of k and K obtained were, respectively, $3.5 \times 10^{-2}\,s^{-1}$ and 1.2×10^4 ($I = 1.3 \times 10^{-2}$ M, $T = 25.0°C$), Fig. 8.

At this pH (4.2) and DPKBH concentration (1.0×10^{-4} M) we consider the primary species ($\approx 70\%$) $[Fe^{II}(RO)(H_2O)]^{2+}$, Fig. 2. As the aqua-complex is significantly more labile (Fig. 7) it is reasonable that at higher HSO_3^- concentration k_{obs1} tends to reach a limiting value. Additionally, although the less reactive species, $[Fe^{III}(RO)_2]^+$ 30%, is present in the proposed scheme, it was not considered in the kinetic treatment because formation of the mixed complex is not favorable.

The formation of $SO_3^{\bullet -}$ radical was considered in the redox process as suggested by many authors [14–16]. The $SO_3^{\bullet -}$ radicals can also decay resulting in formation of $S_2O_6^{2-}$ or can be oxidized to SO_4^{2-} by Fe(III) species.

(b.2) HSO_3^- Concentration Dependence at pH 6.2

At pH 6.2 and 1.0×10^{-4} M DPKBH, $[Fe^{III}(RO)(OH)]^+$ and $[Fe^{III}(RO)_2]^+$ are in the proportions of 70 and 30%, respectively [11], Figs. 7 and 2. The k_{obs1} values increase

with HSO_3^- concentration and depend on the DPKBH concentration, reaching a limiting rate constant due to formation of $[Fe^{III}(RO)(SO_3)]$, Fig. 6(a). As for pH = 4.2, the approach suggested the mechanism described in the following scheme, Eq. (**18**). For 1.0×10^{-4} M DPKBH the values of k and K obtained Eq. (**15**) were $1.4 \times 10^{-2}\,s^{-1}$ and $1.9 \times 10^{2}\,M^{-1}$ ($I = 1.3 \times 10^{-2}$ M, $T = 25.0°C$).

The main products of the redox reaction are SO_4^{2-} and $Fe^{II}(RO)_2]$ which is dominant at DPKBH concentrations $\geq 1.0 \times 10^{-4}$ M [11].

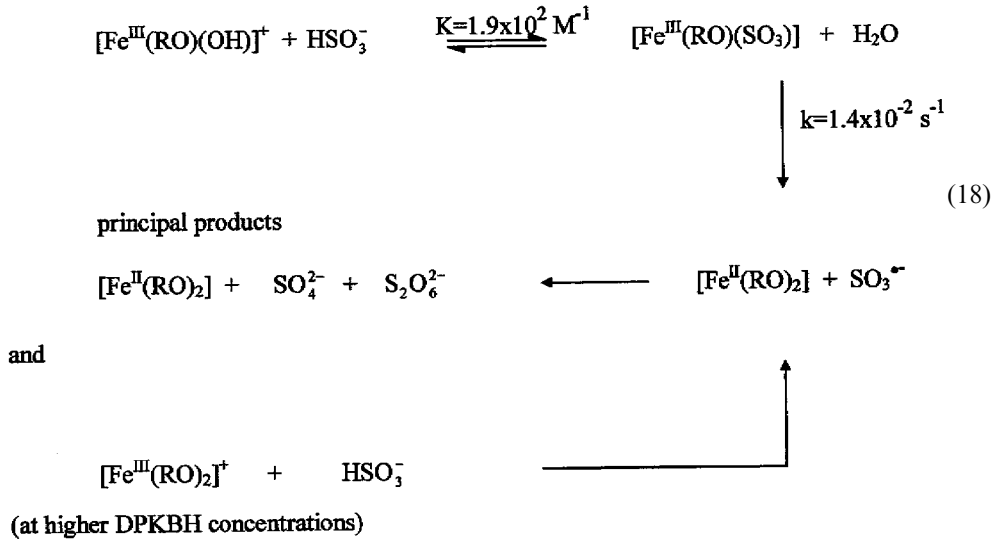

(18)

SCHEME 2 (pH = 6.2).

General Remarks

These studies add information to the qualitative data from Pehkonen *et al.* [1] and outline experimental procedures for Fe(II) and Fe(III) simultaneous determination. Based on our studies we can suggest that, in presence of S(IV), this analytical determination would be more successful if the pH were adjusted around 6.5 (the redox process is slower); even so the absorbance readings should be taken just after mixing the reagents to achieve a smaller analytical error.

Additionally, our studies supplement the equilibrium data for the complexes of Fe(III) with DPKBH from the acid–base equilibrium with the hydrolysis constant determination.

The following scheme (3,4), Eq. (**19**), shows the distribution of the species (acid–base) as a function of pH (4.2 and 6.2).

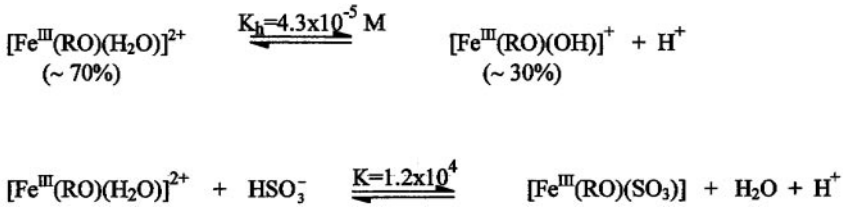

(19)

SCHEME 3 (pH = 4.2).

$$[Fe^{III}(RO)(H_2O)]^{2+} \underset{}{\overset{K_h=4.3\times10^{-5}\ M}{\rightleftharpoons}} [Fe^{III}(RO)(OH)]^{+} + H^{+} \quad (\sim 100\%)$$

$$[Fe^{III}(RO)(OH)]^{+} + HSO_3^{-} \overset{K=1.9\times10^{2}\ M^{-1}}{\rightleftharpoons} [Fe^{III}(RO)(SO_3)] + H_2O$$

SCHEME 4 (pH = 6.2).

The formation of $[Fe^{III}(TH_2)(SO_3)]^{3+}$ [17] (TH_2 = tetraethylenepentamine) and $[Fe^{III}(edta)(SO_3)]^{3-}$ [15] mixed complexes was easily observed by spectral changes. However, in the present work, it was not possible to detect such direct spectral evidence and different values of the mixed complex formation constant were obtained.

The reactions of SO_3^{2-} with $[Fe^{III}(TH_2)]^{5+}$ revealed the existence of two isomers of $[Fe^{III}(TH_2)(SO_3)]^{3+}$ in which SO_3^{2-} is bonded *trans* or *cis* to the coordinated H_2O [17]. It is presumed that coordinated sulfite in the *trans* isomer reduces Fe(III) faster than in the *cis* isomer. Perhaps the k_{obs1} and k_{obs2} values in the present work can be related to *trans* or *cis* complexes.

The reduction of an Fe(III)/edta complex by sulfite was studied in the absence and presence of oxygen [16]. EDTA acts as a hexadentate ligand, however there is evidence of a seven-coordinate species involving a coordinated water molecule, $[Fe^{III}(edta)(H_2O)]^{-}$, with an approximate pentagonal-bipyramidal structure [15]. In the presence of sulfite, $[Fe^{III}(edta)(SO_3)]^{3-}$ is formed and its concentration is controlled by sulfite and H^+ concentration. The decomposition of $[Fe^{III}(edta)(SO_3)]^{3-}$ is strongly dependent on the oxygen concentration. This process occurs by intramolecular electron-transfer reaction and Fe(III) is reduced to Fe(II) and SO_3^{2-} is oxidized to the radical $SO_3^{\bullet-}$. The $[Fe^{II}(edta)]^{2-}$ produced is extremely oxygen sensitive and is rapidly oxidized to $[Fe^{III}(edta)]^{-}$ to complete the redox cycle.

For all of the complexes the results showed the aqua complex as the significantly more labile species.

The hydrolysis constant of $[Fe^{III}(H_2O)_6]^{3+}$ ($K_h = 6.4 \times 10^{-3}$ M at 25°C, $I = 0.1$ M) [18] is ≈150-fold higher than that for $[Fe^{III}(RO)(H_2O)]^{2+}$ ($K_h = 4.3 \times 10^{-5}$ M, present work). This difference may be partially due to an electronic effect, the bound amine ligand probably weakens the Fe^{III}–H_2O bond in $[Fe^{III}(RO)(H_2O)]^{2+}$. The same difference was observed for the $[Fe^{III}(TH_2)(H_2O)_3]^{5+}$ [17].

The values of k_{obs1}, for the further reduction of Fe(III)/DPKBH complexes by sulfite, decreased as pH increased from 4.2 to 7.1 at 6×10^{-4} M HSO_3^- (Fig. 7).

The equilibrium study indicated the presence of $[Fe^{III}(RO)(H_2O)]^{2+}$ and $[Fe^{III}(RO)(OH)]^{+}$ under these pH conditions (Fig. 7).

As discussed earlier, $[Fe^{III}(RO)(OH)]^{+}$ is less reactive. This is in contrast to substitution reactions of $[Fe^{III}(H_2O)_5(OH)]^{2+}$ about 300 times faster [19,20] than for $[Fe^{III}(H_2O)_6]^{3+}$. As for $[Fe^{III}(TH_2)(OH)]^{4+}$ [17], we are led to believe that the reactivity of $[Fe^{III}(RO)(OH)]^{+}$ is considerably reduced suggesting a possible intramolecular hydrogen bonding of the Fe(III)-bound hydroxo group with nitrogen of the ligand.

The reduction of Fe(III) by S(IV) was also studied in presence of tris(1,10-phenanthroline) [21], L, of high acidity (at least 0.05 M), avoiding reaction with OH^-. Some experiments were carried out in excess $[Fe^{III}L_3]^{3+}$ over S(IV) and the aquation

step was faster than in experiments with excess S(IV). The redox mechanism did not consider the solvation and protonation possibilities and the formation of $[Fe^{III}L_2LSO_3]^{2+}$ is postulated as an outer-sphere Fe(III)–S(IV) complex. That work suggested $S_2O_5^{2-}$ may react rapidly in one-electron step and an alternate possibility that decomposition of $[Fe^{III}L_3 \cdot S]^{2+}$ to $[Fe^{II}L_3]^{2+}$ and S(V) can be accelerated by S(IV).

The metal ion catalyzed autoxidation of sulfur(IV)-oxides is shown to be an important reaction step in redox cycling of iron under atmospheric conditions [22–26]. The rate-determining step involves reduction of Fe(III) and oxidation of sulfite to produce the sulfite radical $SO_3^{\bullet -}$, which rapidly reacts with dissolved oxygen to produce $SO_5^{\bullet -}$(and HSO_5^-). The latter species are powerful oxidants and oxidize Fe(II) to Fe(III). When Fe(II) is in large excess there is a net increase in the Fe(III) concentration. The final reaction products are Fe(III) and sulfate which means that Fe(II) and sulfite are oxidized simultaneously by dissolved oxygen. The relative concentrations of HSO_3^- and O_2 determine the oxidation state of the Fe species. Redox cycling with a series of free radical propagation reactions is described in detail [23–26].

Kinetic modeling of the reaction between iron(III) and sulfite ion at large Fe(III) excess showed formation of dinuclear iron(III)–sulfite, $[Fe_2(OH)SO_3]^{3+}$, and mononuclear, $[FeSO_3]^+$ [27,28].

Acknowledgments

The authors gratefully acknowledge financial support from FAPESP (Fundação de Amparo à Pesquia do Estado de São Paulo) and CNPq (Conselho Nacional de Desenvolvimento Científico e Tecnológico).

References

[1] S.O. Pehkonen, Y. Erel and M.R. Hoffmann (1992). *Environ. Sci. Technol.*, **26**, 1731.
[2] T. Nakanishi and M. Otomo (1986). *Microchem. J.*, **33**, 172.
[3] N.A. Zatar, A.Z. Abu-Zuhri, M.A. Al-Nuri, F.M. Mahmoud and A.A. Abu-Obai (1989). *Spectrosc., Lett.*, **22**, 1203.
[4] M.A. Al-Nuri, M. Abu-Eid, N.A. Zatar, S. Khalaf and M. Hannoun (1992). *Anal. Chim. Acta*, **259**, 175.
[5] T.Nakanishi and M. Otomo (1985). *Anal. Sci.*, **1**, 161.
[6] L.H.S. Ávila-Terra, M.R. Hoffmann and M.E.V. Suárez-Iha (1997). *Spectrosc. Lett.*, **30**, 625.
[7] L.H.S. Ávila-Terra, M.C.C. Areias, I. Gaubeur and M.E.V. Suárez-Iha (1999). *Spectrosc. Lett.*, **32**, 257.
[8] A.I. Vogel (1978). *Vogel's Textbook of Quantitative Inorganic Analysis*, 4th edn. Longman Inc., New York.
[9] M. Garcia-Vargas, M. Belizón, M.P. Hernández-Artiga, C. Martinez and J.A. Pérez-Bustamante (1986). *Appl. Spectrosc.*, **40**, 1058.
[10] I. Gaubear, M.V. Rossi, K. Iha and M.E.V. Suárez-Iha (2000). *Eclética Química*, **25**, 63.
[11] M.E.V. Suárez-Iha, S.O. Pehkonen and M.R. Hoffmann (1994). *Environ. Sci. Technol.*, **28**, 2080.
[12] D.A. Skoog, D.M. West and F.J. Holler (1992). *Fundamentals of Analytical Chemistry*, 6th edn. Saunders College Pub., New York.
[13] OLIS KINFIT Routines (1989). ON-Line Instruments Systems, Inc., Jefferson, GA.
[14] H.L.J. Bäckström (1932). *Phys. Chem.*, Abt. **B18**, 103.
[15] M. Dellert-Ritter and R. Van Eldik (1992). *J. Chem. Soc. Dalton*, 1037.
[16] M. Dellert-Ritter and R. Van Eldik (1992). *J. Chem. Soc. Dalton*, 1045.
[17] A.C. Dash, A.K. Patnaik and N. Das (1997). *Indian J. Chem.*, **36A**, 268.
[18] J. Kraft and R. Van Eldik (1989). *Inorg. Chem.*, **28**, 2297.
[19] T.W. Swaddle and A.E. Merbach (1981). *Inorg. Chem.*, **20**, 4212.
[20] A.C. Dash and G.M. Harris (1982). *Inorg. Chem.*, **21**, 1265.
[21] D.W. Carlyle (1972). *J. Am. Chem. Soc.*, **94**, 4525.
[22] P. Behra and L. Sigg (1990). *Nature*, **344**, 419.

[23] K. Bal Reddy, N. Coichev and R. Van Eldik (1991). *J. Chem. Soc., Chem. Commun.*, **481**.
[24] R. Van Eldik, N. Coichev, K. Bal Reddy and A. Gerhard (1992). *Ber. Bunsenges Phys. Chem.*, **96**, 478.
[25] N. Coichev and R. Van Eldik (1994). *New J. Chem.*, **18**, 123.
[26] C. Brandt, I. Fábián and R. Van Eldik (1994). *Inorg. Chem.*, **33**, 687.
[27] G. Lente and I. Fábián (1998). *Inorg. Chem.*, **37**, 4204.
[28] G. Lente and I. Fábián (1999). *Inorg. Chem.*, **38**, 603.